scientific reports

Check for updates

OPEN

Identifying KLF14 as a potential regulatory factor in liver regeneration trough transcriptomic and metabolomic

Chang Liu[1], Dalong Zhu[1], Junlong Xue[1], Alimu Tulahong[1] & Tuerganaili Aji[2]✉

Liver regeneration is a complex process crucial for recovery after partial hepatectomy (PH) or ex-vivo liver resection and autotransplantation (ELRA). This study aimed to explore the molecular mechanisms involved in liver regeneration by analyzing peripheral blood samples from three patients with alveolar echinococcosis undergoing PH and ELRA. Peripheral blood samples were collected from three patients undergoing PH and three patients undergoing ELRA at three time points: pre-operation, postoperative day 1, and postoperative day 5, as well as three healthy controls. Transcriptomic analysis was performed to identify differentially expressed genes (DEGs) using RNA sequencing, while metabolomic analysis was conducted using untargeted liquid chromatography-mass spectrometry (LC–MS). Key findings were validated through real-time quantitative polymerase chain reaction (RT-qPCR) and Western blot analysis. Transcriptomic analysis revealed 3574 DEGs on post-operative day 1 compared to pre-operation in the ELRA group, and 3269 DEGs on post-operative day 5 compared to day 1. In the PH group, 1619 DEGs were identified on post-operative day 1 compared to pre-operation, and 896 DEGs were found on post-operative day 5 compared to day 1. Among these, 36 common genes were shared between both groups, primarily enriched in metabolic pathways. Integration of common genes, co-expression network analysis and Mfuzz clustering identified KLF14 as a gene correlated with liver regeneration processes, with its association with the PI3K-AKT pathway. Metabolomic analysis highlighted differentially expressed metabolites associated with lipid, amino acid, and energy metabolism. This study provides new insights into the molecular regulation of liver regeneration, identifying KLF14 and associated metabolic processes. These findings offer potential therapeutic targets for enhancing liver repair.

Keywords Liver regeneration, Ex-vivo liver resection and autotransplantation, Partial hepatectomy, KLF14, PI3K-AKT

The liver is a unique organ with remarkable regenerative capacity. Liver regeneration is a crucial physiological process in which the liver restores its function through cell proliferation and tissue reconstruction following injury or partial hepatectomy[1]. Alveolar echinococcosis is a zoonotic disease with a global geographical distribution, caused by *Echinococcus multilocularis*[2]. Ex-vivo liver resection and autotransplantation (ELRA) and partial hepatectomy (PH) are the primary surgical methods for treating alveolar echinococcosis[3], and the liver's regenerative ability post-surgery is critical for patient recovery and long-term survival[4]. However, despite the well-recognized clinical importance of liver regeneration, its underlying molecular mechanisms, particularly regarding metabolic and transcriptional regulation, remain poorly understood.

During liver regeneration, hepatocytes must undergo rapid proliferation, metabolic reprogramming, and tissue repair in a short time, processes that are tightly regulated by multiple signaling pathways and metabolic routes[5]. Krüppel-like factors (KLF) are zinc finger domain-containing transcription factors involved in embryonic liver development[6]. Among them, KLF14 is associated with cell proliferation and liver metabolism, reducing the secretion of pro-inflammatory cytokines and lipid accumulation[7]. Moreover, previous studies have shown that signaling pathways such as PI3K-AKT and MAPK play crucial roles in liver cell proliferation and survival, while metabolic pathways involving amino acids, lipids, and glucose metabolism are indispensable in the liver

[1]The First Affiliated Hospital of Xinjiang Medical University, No. 137 Liyushan South Road, Urumqi 830054, Xinjiang, China. [2]Department of Hepatobiliary Hydatid Surgery, The First Affiliated Hospital of Xinjiang Medical University, No. 137 Liyushan South Road, Urumqi 830054, Xinjiang, China. ✉email: tuergan78@sina.com

Variables	Total (n = 39)	Control (n = 13)	PH (n = 13)	ELRA (n = 13)	Statistic	*P*
Age, mean ± SD	58.72 ± 8.54	58.92 ± 9.18	58.85 ± 6.77	58.38 ± 10.03	F = 0.01	0.986
BMI, mean ± SD	23.68 ± 3.03	24.46 ± 3.76	23.08 ± 2.76	23.50 ± 2.51	F = 0.69	0.507
Gender, n (%)					–	1.000
Male	20 (51.28)	6 (46.15)	7 (53.85)	7 (53.85)		
Female	19 (48.72)	7 (53.85)	6 (46.15)	6 (46.15)		

Table 1. General information of the participating population. F: ANOVA; –: Fisher exact; SD: standard deviation

Variables	Total (n = 26)	PH (n = 13)	ELRA (n = 13)	Statistic	*P*
PNM, n (%)				–	0.869
P2N0M0	1 (3.85)	0 (0.00)	1 (7.69)		
P2N1M0	2 (7.69)	2 (15.38)	0 (0.00)		
P3N0 M0	1 (3.85)	1 (7.69)	0 (0.00)		
P3N0M0	3 (11.54)	1 (7.69)	2 (15.38)		
P3N1M0	2 (7.69)	1 (7.69)	1 (7.69)		
P3N1M1	1 (3.85)	0 (0.00)	1 (7.69)		
P4N0M0	10 (38.46)	5 (38.46)	5 (38.46)		
P4N1M0	1 (3.85)	0 (0.00)	1 (7.69)		
P4N1M1	5 (19.23)	3 (23.08)	2 (15.38)		

Table 2. Stage of infections. –: Fisher exact; PNM: Parasile, Neigbbouring organs, and Melaslasis.

regeneration process[8,9]. However, the spatiotemporal dynamics of these processes during liver regeneration, and how transcriptional and metabolic coordination promotes liver regeneration, remain understudied.

To elucidate the molecular mechanisms of liver regeneration following ELRA and PH, this study employed a combination of transcriptomics and untargeted metabolomics (LC–MS) to analyze the dynamic changes in differentially expressed genes and metabolites during the regeneration process at various time points. KLF14 was identified as a key gene, showing dynamic expression patterns across different stages of regeneration. It was found to be correlated with metabolic pathways. Transcriptomic data revealed that genes associated with KLF14 were enriched in pathways related to cell proliferation and immune regulation. Furthermore, metabolomic analysis highlighted shifts in metabolites involved in lipid, amino acid, and glucose metabolism, underscoring the metabolic reprogramming that accompanies liver regeneration. These findings suggest that KLF14 may play an important role in regulating liver regeneration.

Materials and methods

Study subjects

A total of 39 patients were enrolled in this study: 13 patients underwent partial hepatectomy (PH) and 13 patients underwent ex-vivo liver resection and autotransplantation (ELRA), along with 13 healthy controls. The General information of the participating population and stage of infections were shown in Tables 1 and 2. All patients were provided with standardized meals during hospitalization, both preoperatively and postoperatively, ensuring consistency in nutrient intake. Meals were designed to meet clinical nutritional requirements, with controlled macronutrient and micronutrient compositions. Blood samples were collected after an overnight fast (≥ 8 h).

Inclusion criteria: all patients were adults, regardless of gender; participants underwent PH or ELRA based on their clinical treatment plans. All patients underwent comprehensive physiological and pathological evaluations before surgery, including liver ultrasound, contrast-enhanced CT or MRI imaging, liver function tests, coagulation tests, viral hepatitis screening, and liver fibrosis scoring. All patients were clinically diagnosed with alveolar echinococcosis preoperatively and pathologically confirmed postoperatively.

Exclusion criteria: patients with severe underlying liver diseases; those with severe cardiovascular disease, kidney disease, diabetes, or immune system disorders; patients with acute infections, hemorrhagic disorders, hepatorenal syndrome, or other acute complications; patients who had received immunosuppressants or long-term steroid therapy before surgery; and pregnant or breastfeeding women.

All patients provided written informed consent. The study strictly adhered to the Declaration of Helsinki and was approved by the Ethics Committee of the First Affiliated Hospital of Xinjiang Medical University (approval number: 231124-04).

Postoperative follow-up was conducted on postoperative days 1 and 5. On day 1, the initial recovery status was assessed, and peripheral blood samples were collected. On day 5, liver function recovery was further evaluated, potential complications were monitored, and peripheral blood samples were collected again. All samples were processed immediately after collection and stored at −80 °C for transcriptomic and metabolomic analyses.

Transcriptomic sequencing and data preprocessing

To analyze changes in differentially expressed genes (DEGs) during liver regeneration, blood samples of 3 patients underwent PH, 3 patients underwent ELRA, and 3 healthy controls were random selected to extract total RNA using Trizol reagent. The quality of the extracted RNA was measured using a NanoDrop 2000 spectrophotometer (Thermo Scientific), and RNA integrity was confirmed with an Agilent 2100 Bioanalyzer.

High-quality RNA samples were used to construct transcriptomic sequencing libraries, followed by RNA sequencing using the Illumina NovaSeq 6000 platform. Library construction was performed using the Illumina TruSeq RNA Library Preparation Kit (Illumina, San Diego, CA) according to the manufacturer's instructions. The constructed cDNA libraries were subjected to paired-end sequencing on the Illumina NovaSeq 6000 platform, with a sequencing depth of approximately 40–50 million reads per sample. The raw reads obtained from sequencing were first subjected to quality control using FastQC software (v0.11.9). Trimmomatic software (v0.39) was used to remove low-quality reads and adapter sequences. The clean reads were aligned to the human reference genome (GRCh38) using HISAT2 software (v2.1.0), and featureCounts was employed to quantify gene expression for each sample.

Metabolomics analysis

Plasma samples were pre-processed to remove proteins and other interfering substances, and metabolites were analyzed using untargeted liquid chromatography-mass spectrometry (LC–MS). Metabolomic data collection was performed using ultra-high-performance liquid chromatography (UHPLC) coupled with a Thermo Fisher Q Exactive mass spectrometer (LC–MS). An ACQUITY UPLC HSS T3 column (100 mm × 2.1 mm, 1.8 μm) was used as the separation column, with the column temperature set at 40 °C. The mobile phase consisted of solvent A (0.1% formic acid in water) and solvent B (0.1% formic acid in acetonitrile). A gradient elution method was used, with a flow rate of 0.3 mL/min, and a sample injection volume of 5 μL. The mass spectrometer operated in both positive and negative ion modes, utilizing full scan and data-dependent acquisition (DDA) modes. The mass range was set to m/z 100–1500.

The LC–MS data were pre-processed using CD3.3 data processing software. Metabolites were quantified with CD3.3 software. Metabolite identification was performed by comparing the high-resolution MS/MS spectra against the mzCloud and mzVault databases, as well as the MassList primary database.

Differential expression and enrichment analysis

Gene expression differences between preoperative and postoperative time points were analyzed using DESeq2 software (v1.30.0). Differentially expressed genes (DEGs) were defined with a threshold of p value < 0.05 and |log2FoldChange| ≥ 1.

Partial least squares discriminant analysis (PLS-DA) was applied to the metabolomic data, and differential metabolites were selected based on the Variable Importance in the Projection (VIP) value, with VIP > 1 and $p < 0.05$ as the criteria for significance.

The Gene Ontology (GO) and Kyoto Encyclopedia of Genes and Genomes (KEGG) pathway[10] enrichment analysis for DEGs was conducted using the clusterProfiler package.

Time-series clustering and co-expression analysis

Time-series clustering of DEGs was performed using the Mfuzz software package[11] to identify gene expression patterns related to liver regeneration at different postoperative time points.

Weighted Gene Co-expression Network Analysis (WGCNA) was used to construct a co-expression network for genes with variability greater than 5000, and gene modules significantly associated with liver regeneration were identified.

Real-time quantitative polymerase chain reaction (RT-qPCR)

Total RNA was extracted from blood samples of remaining 10 patients underwent PH, 10 patients underwent ELRA, and 10 healthy controls using Trizol reagent (Thermo Fisher Scientific). The concentration and purity of the RNA were measured using a NanoDrop 2000 spectrophotometer (Thermo Fisher Scientific). The extracted RNA was then reverse transcribed into cDNA using the High-Capacity cDNA Reverse Transcription Kit (Applied Biosystems). RT-qPCR was performed using the SYBR Green detection system on an Applied Biosystems 7500 real-time PCR system. The specific primer sequences are listed in Table S1. Relative expression levels of the target genes were calculated using the $2^{-\Delta\Delta Ct}$ method, with GAPDH serving as the internal control.

Western blot

Blood samples of remaining 10 patients underwent PH, 10 patients underwent ELRA, and 10 healthy controls were incubated with cold RIPA buffer containing protease inhibitors for 30 min. The lysed samples were centrifuged at 14,000 rpm for 15 min at 4 °C, and the supernatant containing total protein was collected. Protein concentration for each sample was quantified using a BCA Protein Assay Kit (Thermo Fisher Scientific). Protein samples (20 μg) were loaded onto a 10% SDS-PAGE gel for electrophoresis and subsequently transferred to a pre-activated PVDF membrane (Millipore). The membrane was blocked in 5% non-fat milk at room temperature for 1 h. KLF14 (Abcam, 1:1000 dilution), AKT (Abcam, 1:1000 dilution), p-AKT (Abcam, 1:1000 dilution), PI3K (Abcam, 1:1000 dilution), p-PI3K (ABclonal, 1:2000 dilution) primary antibodies were incubated with the membrane overnight at 4 °C. After washing, the membrane was incubated with horseradish peroxidase (HRP)-conjugated secondary antibodies (Abcam, 1:5000 dilution) at room temperature for 1 h. Enhanced chemiluminescence (ECL, Thermo Fisher Scientific) was used for signal detection, and the signals were captured using the Bio-Rad ChemiDoc MP imaging system. Protein expression levels were normalized to β-actin as the internal control, and ImageJ software was used for quantitative analysis of the protein bands.

Statistical analysis

Bioinformatics analysis was performed using R 4.2, and statistical analysis of experimental data was carried out using GraphPad Prism 9 software. Data are presented as mean ± standard deviation (SD). Differences between time points were analyzed using one-way analysis of variance (ANOVA) or t-tests. A p-value of less than 0.05 was considered statistically significant.

Ethics approval

This study was approved by Ethics Committee of the First Affiliated Hospital of Xinjiang Medical University (No. 231124-04).

Results

Identification of differentially expressed genes

We compared gene expression levels at different postoperative time points and identified a large number of DEGs related to liver regeneration. In the ELRA group, 3574 DEGs were identified on postoperative day 1 compared to preoperative levels (Fig. 1A). Additionally, 3269 DEGs were identified when comparing postoperative day 5 to day 1 (Fig. 1B). In the PH group, 1619 DEGs were identified on postoperative day 1 compared to preoperative levels (Fig. 1C), and 896 DEGs were identified when comparing postoperative day 5 to day 1 (Fig. 1D). Further analysis revealed 36 common genes shared between the ELRA and PH groups (Fig. 1E, Table S1).

The common genes identified were enriched in several biological processes related to immune response and cell migration, such as humoral immune response, neutrophil migration, and leukocyte mediated immunity, indicating that the immune system plays a significant role in liver regeneration (Fig. 2A). The KEGG pathway enrichment showed that common genes were heavily reliant on metabolic reprogramming, as seen by the strong enrichment in Metabolic pathways, Nitrogen metabolism, and Fructose and mannose metabolism (Fig. 2B).

Time series clustering analysis

Using the Mfuzz software, time-series clustering analysis of transcriptomic data was performed to further reveal gene expression patterns at different time points. The results identified eight distinct gene clusters (C1 to C8) through Mfuzz time-series clustering during liver regeneration following ELRA (Fig. 3). We found that cluster C8 is closely associated with the liver regeneration process post-ELRA. Genes in cluster C8 were upregulated on postoperative day 1 and gradually decreased by day 5, suggesting that these genes may play key roles in the early stages of liver regeneration.

Additionally, eight distinct gene clusters (C1 to C8) were identified during liver regeneration following PH (Fig. 4). Cluster C1 was found to be associated with liver regeneration after PH. Genes in cluster C1 were

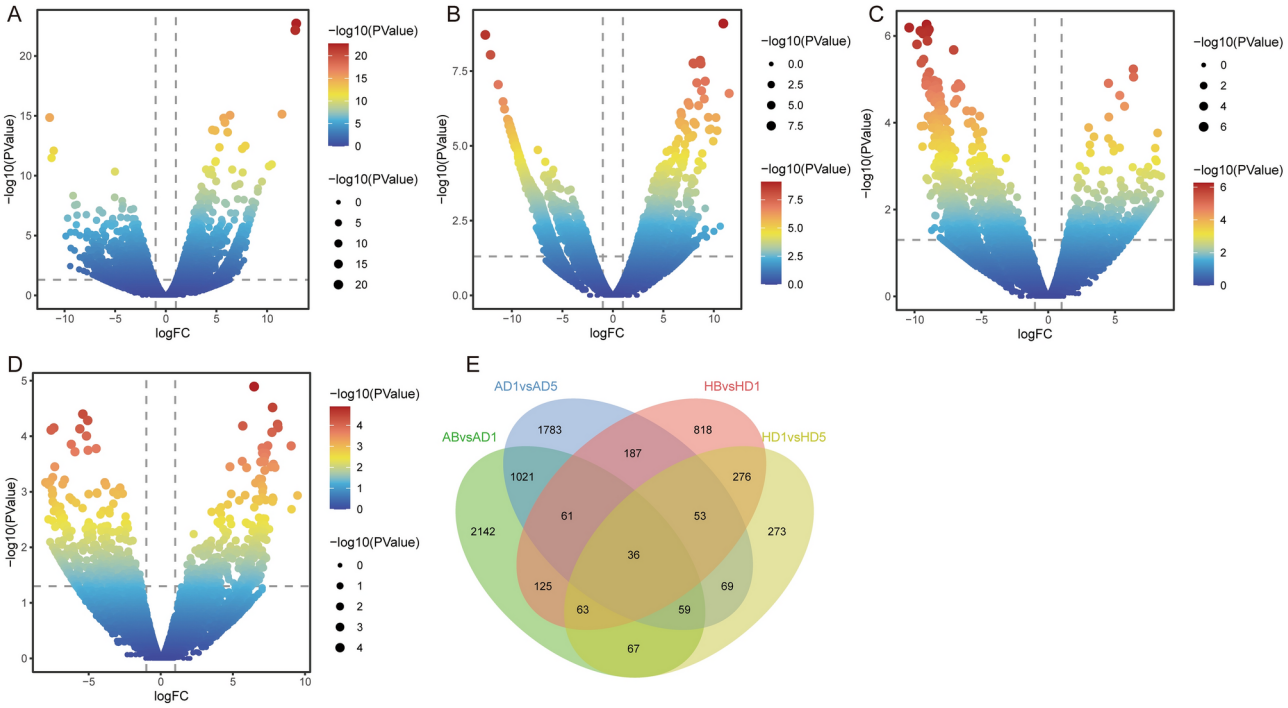

Fig. 1. Identification of differentially expressed genes in ELRA and PH. (**A**) Volcanic plot of differentially expressed genes between postoperative day 1 and preoperative ELRA. (**B**) Volcano plot of differentially expressed genes between postoperative day 5 and day 1 in ELRA. (**C**) Volcanic plot of differentially expressed genes between postoperative day 1 and preoperative PH. (**D**) Volcanic plot of differentially expressed genes between postoperative day 5 and day 1 in PH. (**E**) The intersection of four differentially expressed genes.

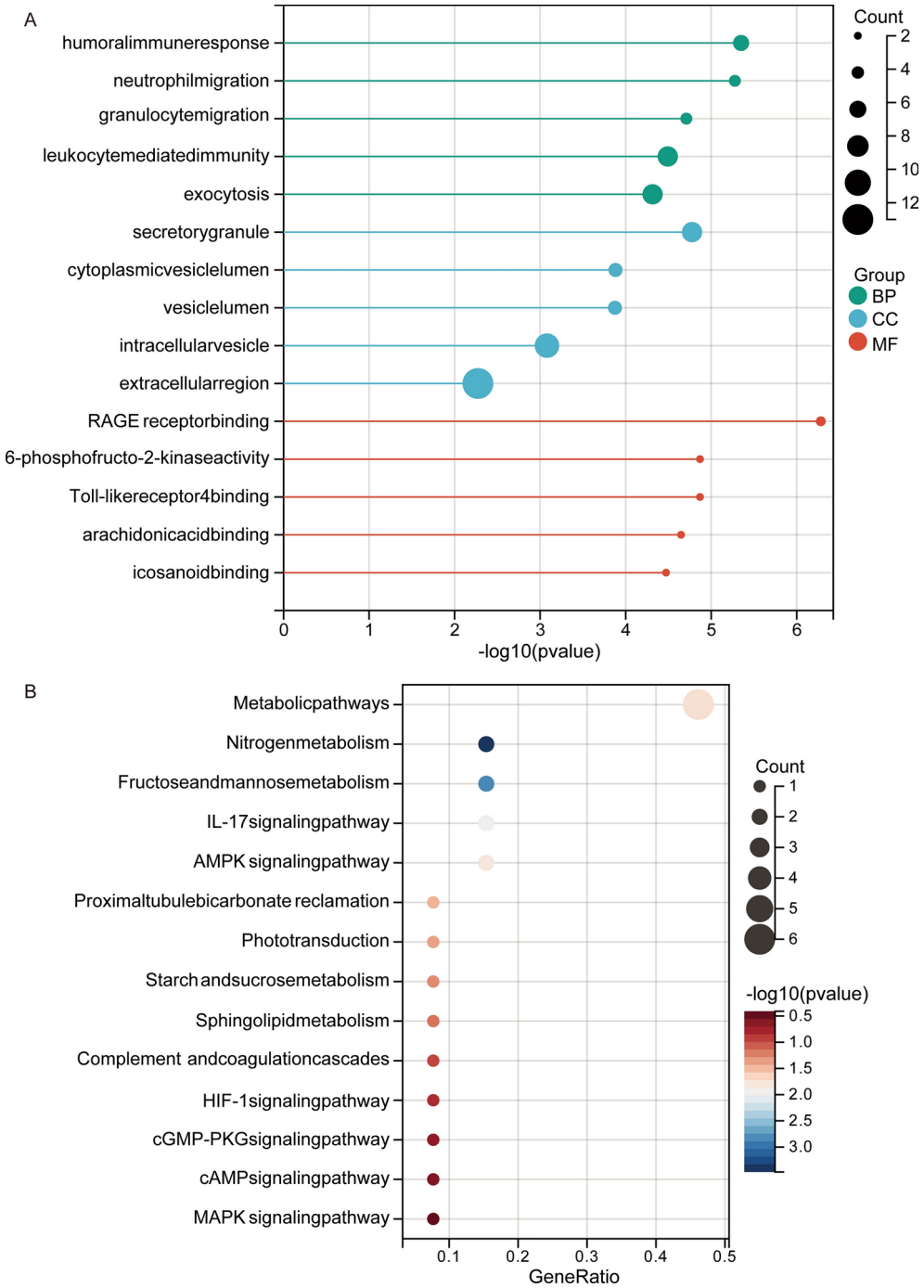

Fig. 2. GO and KEGG enrichment analysis of common genes involved in ELRA and PH. (**A**) Gene Ontology (GO) enrichment analysis of the common genes, including Biological Processes (BP, green), Cellular Components (CC, blue), and Molecular Functions (MF, red). (**B**) Kyoto Encyclopedia of Genes and Genomes (KEGG) pathway enrichment analysis of common genes.

significantly upregulated on postoperative day 1 and showed a decline in expression by day 5, indicating that these genes may be involved in the early recovery process after partial hepatectomy.

KEGG enrichment analysis for the C8 genes in ELRA, which is significantly associated with early liver regeneration, like PI3K-Akt signaling pathway, MAPK signaling pathway, and Rap1 signaling pathway (Fig. 5A). The KEGG analysis for the C1 genes in PH, which is more associated with later stages of liver regeneration, shows a strong enrichment in metabolic pathways and purine metabolism (Fig. 5B).

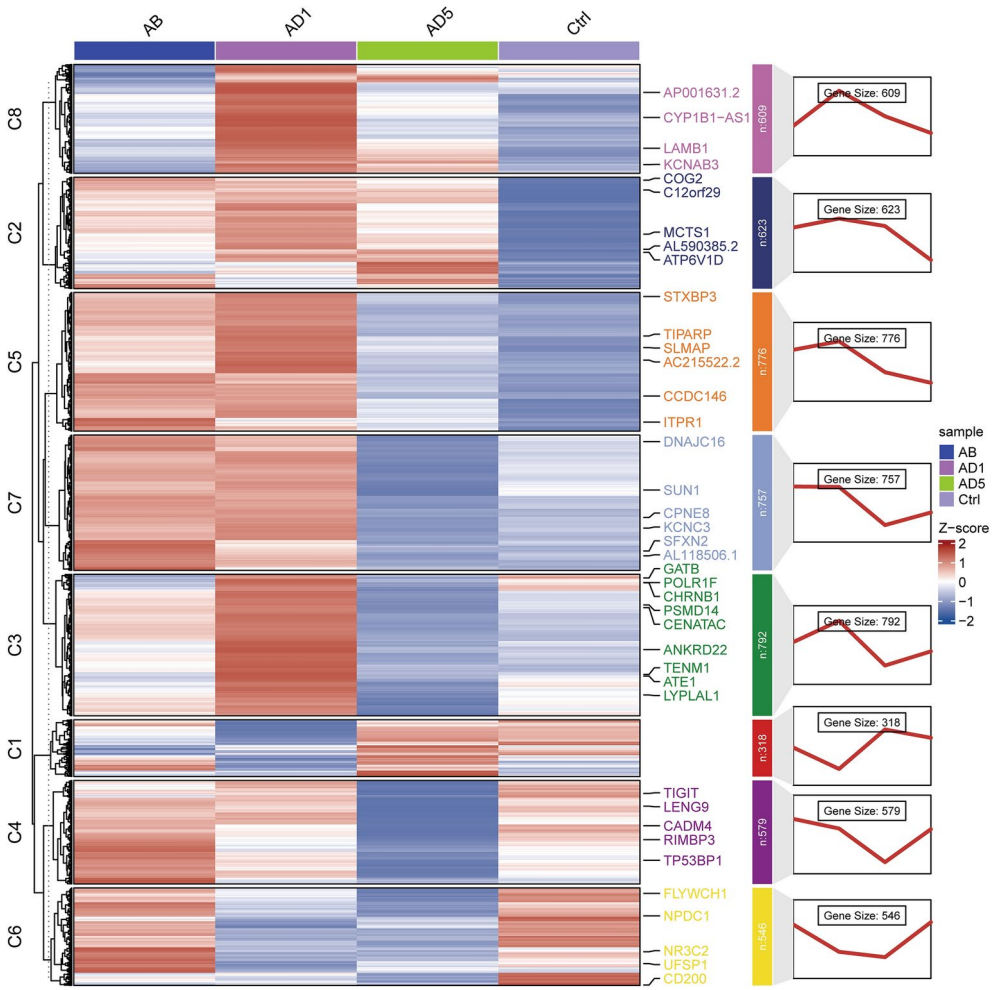

Fig. 3. Time-series clustering analysis of gene expression during liver regeneration in ELRA using Mfuzz.

Gene co-expression network analysis

To further understand the synergistic role of genes during liver regeneration, we employed Weighted Gene Co-expression Network Analysis (WGCNA) to construct a co-expression network. The hierarchical clustering dendrogram, combined with dynamic tree cutting, identified 12 gene co-expression modules (shown in different colors). These modules represent groups of genes with similar expression patterns throughout the liver regeneration process (Fig. 6A, Table S2). The heatmap of module-trait relationships (Fig. 6B) provided valuable insights into the correlation between gene modules and clinical traits. We found that genes in the blue module were significantly negatively correlated with the liver regeneration process.

Importantly, by comparing genes from the blue module with the common genes, C8 genes in ELRA, and C1 genes in PH, we further identified KLF14 as a key regulatory gene involved in liver regeneration (Fig. 6C). As a potential association between KLF14 and the PI3K-AKT signaling pathway, highlighting its potential role as a regulator in the liver regeneration process.

Metabolomics analysis results

Metabolomics analysis using untargeted liquid chromatography-mass spectrometry (LC–MS) revealed significant changes in metabolite expression during liver regeneration following ELRA and PH. On postoperative day 1 after ELRA, 196 differentially expressed metabolites were identified compared to preoperative levels (Figure S1A, B), including arachidic acid, serotonin, and taurine. When comparing postoperative day 5 to day 1, 33 differentially expressed metabolites were identified (Figure S1C, D), including punicic acid, kojic acid, and L-Lysine. Correlation analysis shows that KLF14 is significantly positively correlated with Kojic acid and significantly negatively correlated with Serotonin (Figure S1E). Enrichment analysis revealed that differentially expressed metabolites are mainly involved in lipid metabolism, amino acid metabolism, and energy metabolism (Figure S2A, B, C).

For PH, 82 differentially expressed metabolites were identified on postoperative day 1 compared to preoperative levels (Figure S3A, B), including deoxycholic acid, LPC (18:1), and arachidonic acid. Additionally, 75 differentially expressed metabolites were identified when comparing postoperative day 5 to day 1 (Figure S3C, D), including corticosterone, prostaglandins, and 5-Hydroxytryptophan. Correlation analysis shows that KLF14

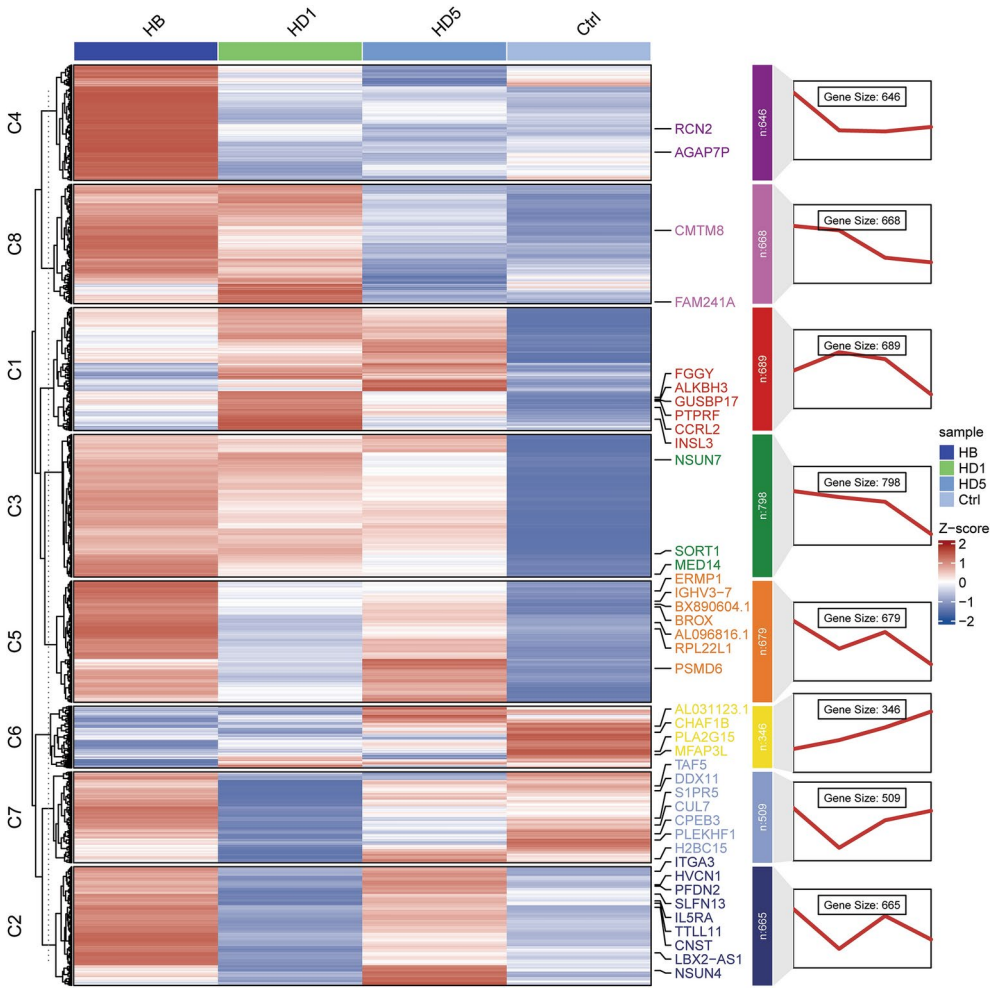

Fig. 4. Time-series clustering analysis of gene expression during liver regeneration in PH using Mfuzz.

is significantly positively correlated with Prostaglandin H1 and significantly negatively correlated with LPC 18:1 (Figure S3E). Enrichment analysis revealed that differentially expressed metabolites are also mainly involved in lipid metabolism, amino acid metabolism, and energy metabolism (Figure S4A, B, C).

Verification of KLF14 and signaling pathways

To verify the role of KLF14 in liver regeneration, we examined the expression levels of KLF14 and its associated signaling pathways using RT-qPCR and Western blot techniques. RT-qPCR results showed that KLF14, AKT, and PI3K were significantly upregulated on postoperative days 1 and 3 in both ELRA and PH, and their expression decreased by day 5 (Fig. 7). Western blot analysis further confirmed the activation of KLF14 in the PI3K-AKT signaling pathway on postoperative day 1 in both ELRA and PH, with a marked reduction in activity by day 5 (Fig. 8, Figure S5).

Discussion

This study systematically integrated transcriptomic and metabolomic data to reveal the dynamic changes in gene expression and metabolite profiles during liver regeneration following ELRA and PH, identifying key molecular mechanisms and metabolic reprogramming closely related to liver regeneration. We found distinct differences in gene expression patterns and metabolic characteristics during early and late regeneration stages between ELRA and PH, indicating that liver regeneration involves time-dependent molecular regulation.

Firstly, differential analysis revealed a large number of DEGs after ELRA and PH, but the gene expression patterns differed significantly. Compared to ELRA, the regenerative response following PH showed smaller fluctuations in gene expression, suggesting that the physiological mechanisms of liver regeneration after partial hepatectomy are more stable, with a critical dependence on energy metabolism.

Further analysis of the 36 common genes indicated enrichment in biological processes related to immune response and cell migration, particularly humoral immune response, neutrophil migration, and leukocyte-mediated immune responses, highlighting the important regulatory role of the immune system in liver regeneration[12,13]. Previous studies have also demonstrated that liver regeneration depends not only on local cell proliferation but also on the coordinated regulation of the systemic immune system to prevent tissue

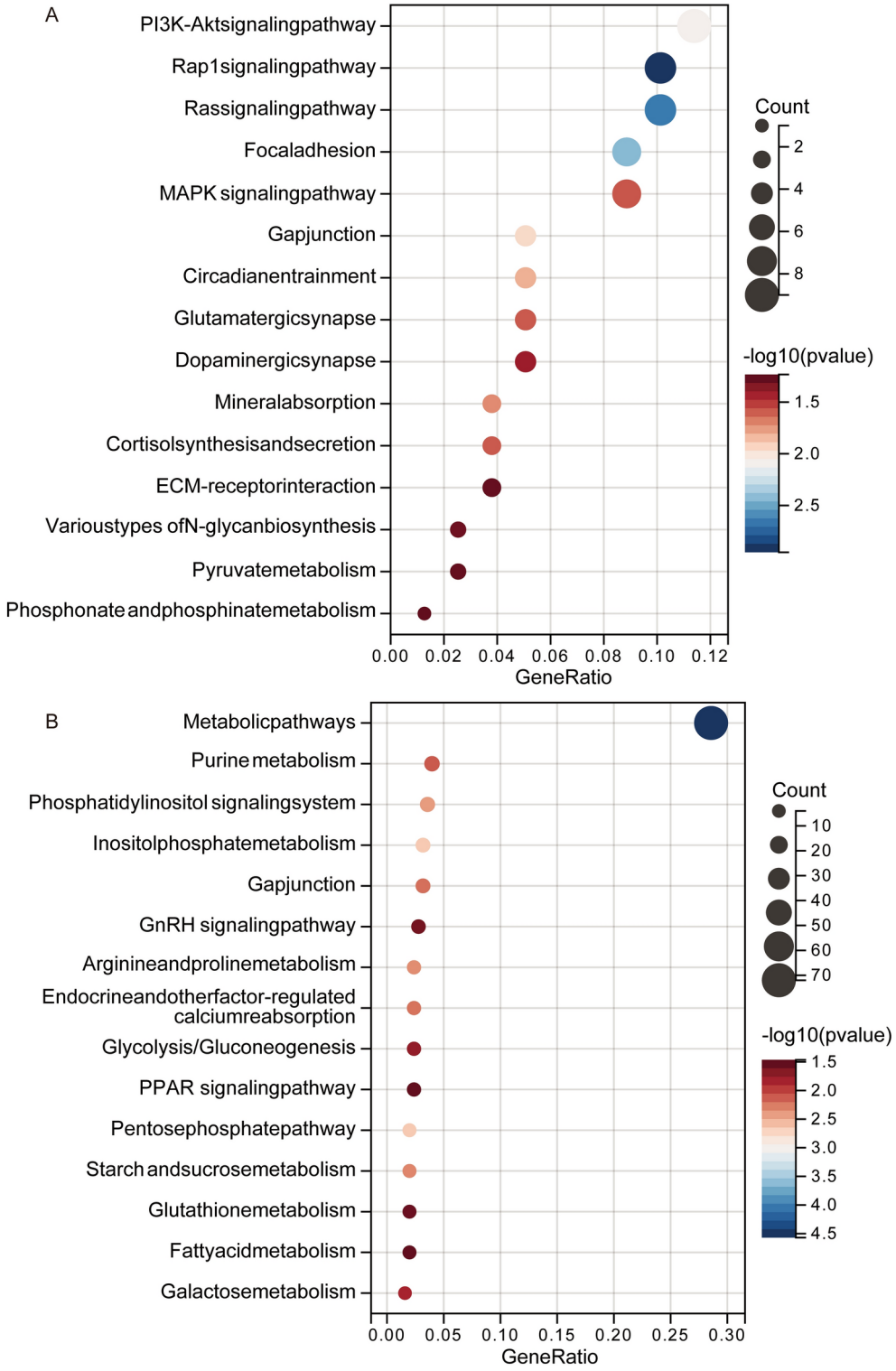

Fig. 5. KEGG enrichment analysis for C8 in ELRA and C1 in PH. (**A**) KEGG pathway enrichment analysis for genes in cluster C8. (**B**) KEGG pathway enrichment analysis for genes in cluster C1.

damage, infection, and promote resolution of inflammation[14,15]. Additionally, KEGG pathway enrichment analysis revealed that these common genes were closely related to metabolic reprogramming, especially in key pathways such as nitrogen metabolism, fructose, and mannose metabolism[16,17]. These results indicate that liver regeneration is not just a local repair process but also involves widespread systemic metabolic regulation to support cell proliferation and organ function restoration[18].

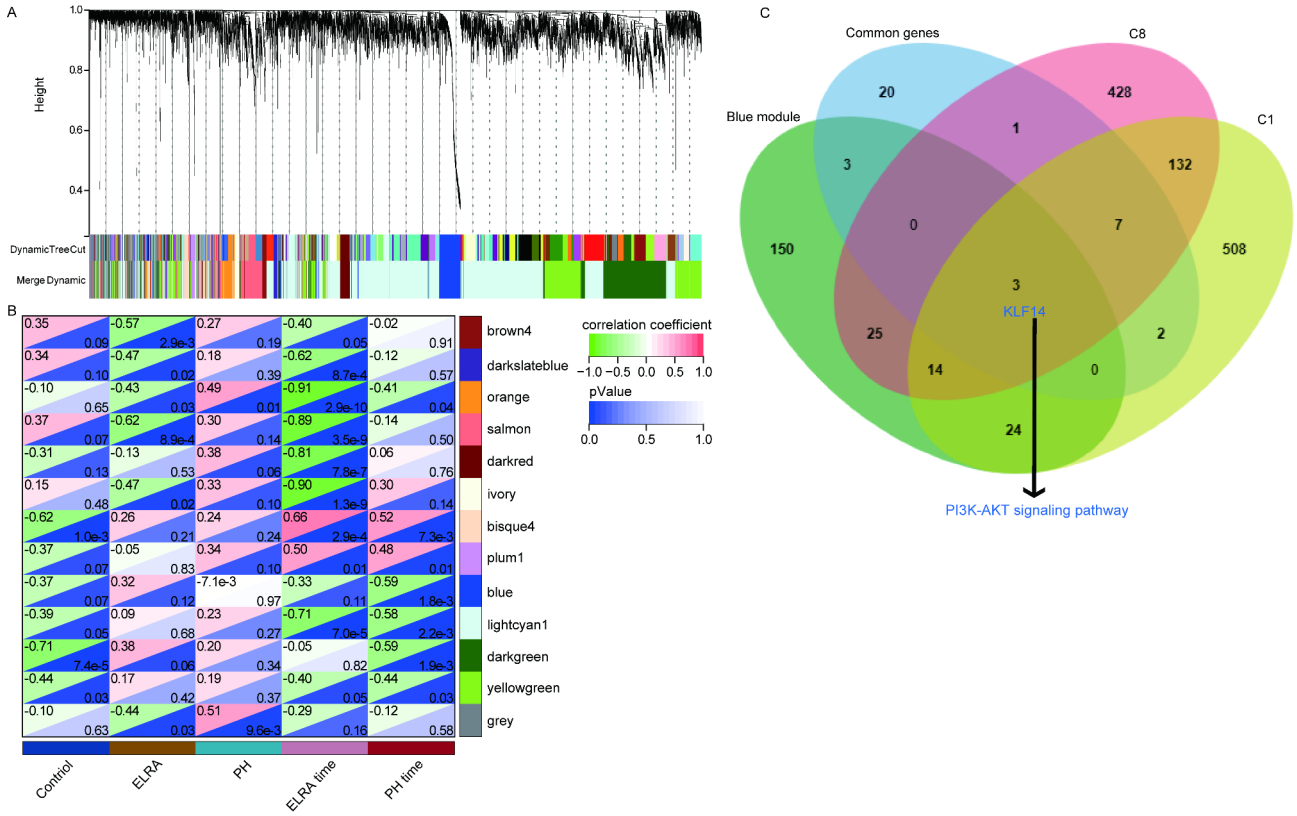

Fig. 6. Weighted Gene Co-expression Network Analysis (WGCNA) of gene modules in liver regeneration. (**A**) Hierarchical clustering dendrogram showing gene modules identified using WGCNA. (**B**) Module-trait relationships. The heatmap displays the correlation coefficients (top half of each cell) and corresponding p-values (bottom half of each cell) between the identified gene modules and clinical traits, including control, ELRA, PH, ELRA time points, and PH time points. **(C)** KLF14 was identified key regulatory gene involved in liver regeneration.

Time-series clustering analysis with Mfuzz revealed the dynamic patterns of gene expression at different time points, further exploring the spatiotemporal regulation during liver regeneration. In the ELRA group, genes in cluster C8 were significantly upregulated on postoperative day 1 and gradually downregulated by day 5, suggesting that these genes play a central role in the early stages of liver regeneration. These genes are involved in key signaling pathways such as PI3K-AKT, MAPK, and Rap1, indicating their crucial roles in regulating cell proliferation, survival, and metabolic reprogramming[19,20]. In contrast, in PH, genes in cluster C1 were significantly upregulated on postoperative day 1, with decreased expression by day 5, indicating their involvement in energy metabolism and tissue repair[21,22], with metabolic demands different from those in ELRA. The significant enrichment of metabolic pathways, including purine metabolism, in PH highlights energy supply and cellular metabolism as key limiting factors in the regeneration process following partial hepatectomy[23–25].

To further understand the synergistic roles of these genes, we constructed a co-expression network using WGCNA, identifying 12 gene modules with significant co-expression relationships. Among them, the blue module was negatively correlated with liver regeneration, suggesting that these genes may be suppressed or involved in negative feedback regulation after liver injury. By comparing with common genes, C8 cluster genes, and C1 cluster genes, we identified KLF14 within the blue module provide insights into the potential involvement of KLF14 in liver regeneration. KLF14 is a known transcription factor involved in regulating metabolism and cell proliferation[26,27]. This study further confirmed its role in liver regeneration through the PI3K-AKT signaling pathway. The upregulation of KLF14 was closely associated with the activation of the PI3K-AKT pathway, which has been widely reported to play a critical role in controlling cell proliferation, survival, and metabolism[28]. Thus, KLF14 may promote liver regeneration and repair by regulating these processes.

Metabolomics analysis further revealed significant changes in metabolites during liver regeneration following ELRA and PH. After ELRA, metabolites such as arachidonic acid, serotonin, and taurine were significantly upregulated in the early phase, suggesting their involvement in inflammation regulation and cell proliferation[29,30]. By postoperative day 5, metabolites such as punicic acid and L-lysine showed significant changes, reflecting evolving metabolic demands during liver regeneration. These metabolites are related to lipid metabolism and amino acid metabolism, indicating that metabolic regulation during regeneration involves not only energy supply but also membrane synthesis and protein production[31,32]. After PH, the upregulation of metabolites such as deoxycholic acid and LPC (18:1) suggests that bile acid and lipid metabolism play a role in liver repair, while changes in corticosterone and prostaglandin levels on postoperative day 5 reflect continued immune regulation

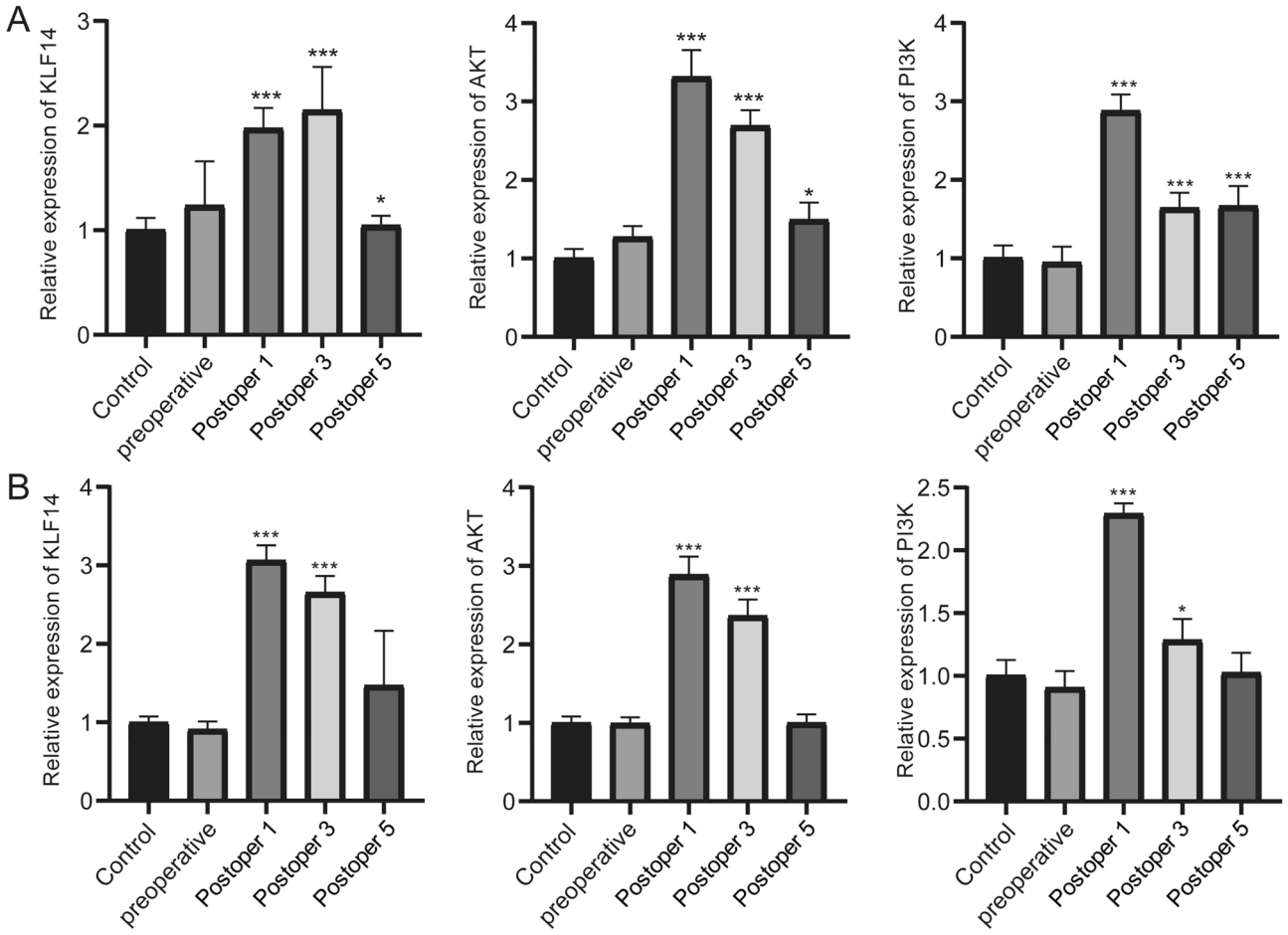

Fig. 7. RT-qPCR analysis of KLF14, PI3K, and AKT mRNA levels. The mRNA levels before and after ELRA (**A**) and PH (**B**) surgery. $^{*}P<0.05$, $^{***}P<0.001$.

and tissue repair[33–35]. These metabolic changes highlight the importance of metabolic reprogramming during liver regeneration, especially in different stages of energy metabolism and inflammation regulationy[23,36,37].

To validate the function of KLF14 in liver regeneration, we assessed its expression levels and associated signaling pathways using RT-qPCR and Western blot analysis. RT-qPCR results showed that KLF14, and PI3K-AKT signaling pathway were significantly upregulated on postoperative day 1 in both ELRA and PH, with a reduction in expression by day 5, highlighting the importance of these genes in early regeneration. Western blot analysis further confirmed the dynamic expression of KLF14 in liver regeneration, with a marked increase in pathway activity on postoperative day 1. This finding provides new evidence supporting the critical role of KLF14 as a regulatory factor in liver regeneration, suggesting its potential as a therapeutic target for promoting cell proliferation and metabolic remodeling.

This study has several limitations. It included a small number of ELRA and PH patients, and the small sample size may affect the generalizability and statistical robustness of the findings. These conclusions should be considered preliminary. The observed associations, particularly the involvement of KLF14, require further validation in larger cohorts to assess their generalizability and statistical significance. The samples were primarily derived from PBMCs rather than directly from liver tissue. Blood samples reflect systemic changes in gene expression, which may not always correlate with local changes in the liver, changes in liver-specific cell types, such as hepatocytes, are not directly reflected in blood samples. Important regulatory genes specific to the liver's regenerative processes might be underrepresented or not detected in blood samples, and there is a lack of spatial resolution needed to assess specific regions of the liver or track dynamic changes in gene expression at different stages of regeneration. Additionally, this study focused on three time points: preoperative, postoperative day 1, and postoperative day 5, which do not comprehensively capture the dynamic changes throughout the entire liver regeneration process. The stage of infection may have influenced the baseline liver function and regenerative capacity, with more advanced stages potentially altering both the inflammatory response and metabolic reprogramming. Although we validated KLF14 expression through RT-qPCR and Western blot, functional studies such as gene knockout or overexpression experiments in vitro or in vivo are still lacking to directly verify its precise role in liver regeneration. We acknowledge that complete dietary control outside the hospital environment is challenging, and unaccounted dietary differences might contribute to minor variations in metabolite profiles. However, the observed trends in key metabolic pathways were consistent across patients and

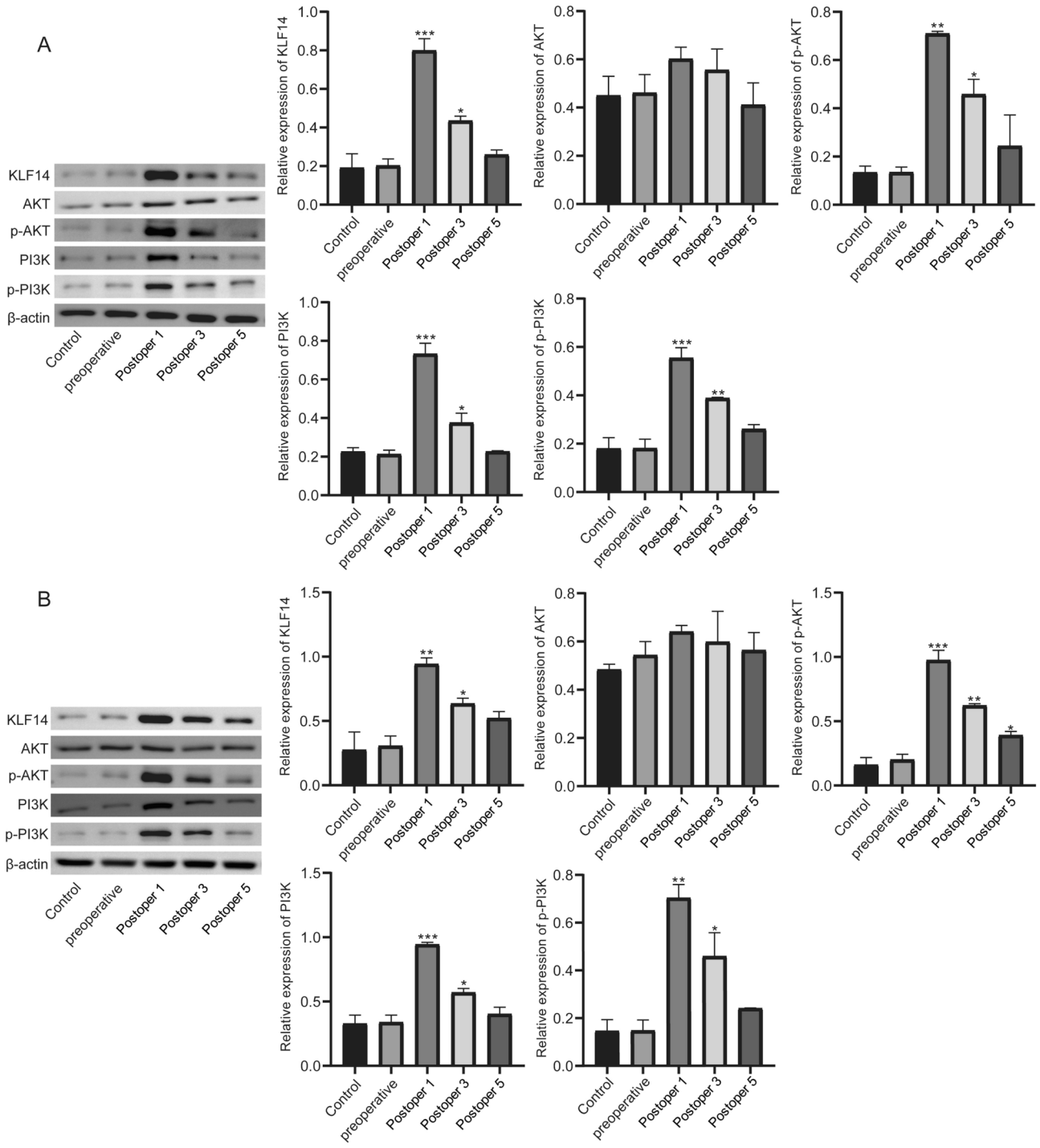

Fig. 8. Western blot analysis of KLF14 and PI3K-AKT pathway protein expression levels. The protein expression levels before and after ELRA (**A**) and PH (**B**) surgery. Original blots are presented in Figure S5. $^{*}P<0.05$, $^{**}P<0.01$, $^{***}P<0.001$.

time points, supporting the robustness of the findings. Future research should expand the sample size, increase the number of time points for analysis, conduct functional validation experiments, and incorporate liver tissue samples for more in-depth investigation.

Conclusion

Through integrated transcriptomic and metabolomic analyses, we systematically revealed the complex gene and metabolic regulatory networks involved in liver regeneration following ex-vivo liver resection and autotransplantation and partial hepatectomy. The identification of KLF14 as a key regulatory factor offers new

insights into the molecular mechanisms of liver regeneration, particularly in the regulation of the PI3K-AKT signaling pathway. This research not only provides important molecular targets for fundamental studies on liver regeneration but also holds potential clinical value for the development of future interventions to promote liver regeneration.

Data availability

The datasets generated and/or analysed during the current study are available in the NCBI repository, [accession number: PRJNA1174874].

Received: 8 October 2024; Accepted: 21 January 2025
Published online: 03 March 2025

References

1. Liu, Q. et al. Liver regeneration after injury: Mechanisms, cellular interactions and therapeutic innovations. *Clin. Transl. Med.* **14**(8), e1812 (2024).
2. McManus, D. P., Gray, D. J., Zhang, W. & Yang, Y. Diagnosis, treatment, and management of echinococcosis. *BMJ* **344**, e3866 (2012).
3. Wen, H., Vuitton, L. & Tuxun, T. et al. Echinococcosis: Advances in the 21st century. *Clin. Microbiol. Rev.* **32**(2), e00075-18 (2019).
4. Yagi, S., Hirata, M., Miyachi, Y. & Uemoto, S. Liver regeneration after hepatectomy and partial liver transplantation. *Int. J. Mol. Sci.* **21**(21), 8414 (2020).
5. Rodimova, S. et al. Effect of hepatic pathology on liver regeneration: The Main metabolic mechanisms causing impaired hepatic regeneration. *Int. J. Mol. Sci.* **24**(11), 9112 (2023).
6. Oishi, Y. & Manabe, I. Kruppel-like factors in metabolic homeostasis and cardiometabolic disease. *Front. Cardiovasc. Med.* **5**, 69 (2018).
7. Yerra, V. G. & Drosatos, K. Specificity proteins (SP) and Kruppel-like factors (KLF) in liver physiology and pathology. *Int. J. Mol. Sci.* **24**(5), 4682 (2023).
8. Kiseleva, Y. V. et al. Molecular pathways of liver regeneration: A comprehensive review. *World J. Hepatol.* **13**(3), 270–290 (2021).
9. Sun, R. et al. The integrated analysis of gut microbiota and metabolome revealed steroid hormone biosynthesis is a critical pathway in liver regeneration after 2/3 partial hepatectomy. *Front. Pharmacol.* **15**, 1407401 (2024).
10. Kanehisa, M. & Goto, S. KEGG: Kyoto encyclopedia of genes and genomes. *Nucleic Acids Res.* **28**(1), 27–30 (2000).
11. Kumar, L. & Futschik, M. E. Mfuzz: A software package for soft clustering of microarray data. *Bioinformation* **2**(1), 5–7 (2007).
12. Getter, T. et al. Novel inhibitors of leukocyte transendothelial migration. *Bioorg. Chem.* **92**, 103250 (2019).
13. Jaeschke, H. & Smith, C. W. Cell adhesion and migration. III. Leukocyte adhesion and transmigration in the liver vasculature. *Am. J. Physiol.* **273**(6), G1169–G1173 (1997).
14. Duan, M. et al. Orchestrated regulation of immune inflammation with cell therapy in pediatric acute liver injury. *Front. Immunol.* **14**, 1194588 (2023).
15. Cooke, J. P. & Lai, L. Transflammation in tissue regeneration and response to injury: How cell-autonomous inflammatory signaling mediates cell plasticity. *Adv. Drug Deliv. Rev.* **203**, 115118 (2023).
16. Hong, J. G., *et al*. Mannose supplementation curbs liver steatosis and fibrosis in murine MASH by inhibiting fructose metabolism. bioRxiv (2024).
17. Ghafoory, S. et al. Zonation of nitrogen and glucose metabolism gene expression upon acute liver damage in mouse. *PLoS One.* **8**(10), e78262 (2013).
18. Paneda, C. et al. Liver cell proliferation requires methionine adenosyltransferase 2A mRNA up-regulation. *Hepatology* **35**(6), 1381–1391 (2002).
19. Abedi-Valugerdi, M., Zheng, W., Benkessou, F., Zhao, Y. & Hassan, M. Differential effects of low-dose fludarabine or 5-fluorouracil on the tumor growth and myeloid derived immunosuppression status of tumor-bearing mice. *Int. Immunopharmacol.* **47**, 173–181 (2017).
20. Liu, C., Cao, Y. P., Yang, X., Mashiba, T. & Mori, S. Long-term and high-dose bisphosphonate administration causes no bone over-mineralization. *Zhonghua Yi Xue Za Zhi.* **89**(42), 2968–2971 (2009).
21. Rajcsanyi, L. S. et al. Genetic variants in genes involved in creatine biosynthesis in patients with severe obesity or anorexia nervosa. *Front. Genet.* **14**, 1128133 (2023).
22. Ma, L. et al. Adipsin and adipocyte-derived C3aR1 regulate thermogenic fat in a sex-dependent fashion. *JCI Insight* **9**(11), e178925 (2024).
23. Alexandrino, H. et al. Mitochondrial bioenergetics and posthepatectomy liver dysfunction. *Eur. J. Clin. Invest.* **46**(7), 627–635 (2016).
24. Kerem, M. et al. Ischemic preconditioning improves liver regeneration by sustaining energy metabolism after partial hepatectomy under ischemia in rats. *Liver Int.* **26**(8), 994–999 (2006).
25. Mann, D. V. et al. Human liver regeneration: Hepatic energy economy is less efficient when the organ is diseased. *Hepatology* **34**(3), 557–565 (2001).
26. Akash, M. S. H. et al. Biochemical activation and regulatory functions of trans-regulatory KLF14 and its association with genetic polymorphisms. *Metabolites* **13**(2), 199 (2023).
27. Zhou, H. et al. KLF14 regulates the growth of hepatocellular carcinoma cells via its modulation of iron homeostasis through the repression of iron-responsive element-binding protein 2. *J. Exp. Clin. Cancer Res.* **42**(1), 5 (2023).
28. Yang, M. et al. Kruppel-like factor 14 increases insulin sensitivity through activation of PI3K/Akt signal pathway. *Cell Signal.* **27**(11), 2201–2208 (2015).
29. Aradhyula, V. et al. Transcriptomic analysis of arachidonic acid pathway genes provides mechanistic insight into multi-organ inflammatory and vascular diseases. *Genes (Basel)* **15**(7), 954 (2024).
30. Jang, Y., Kim, M. & Hwang, S. W. Molecular mechanisms underlying the actions of arachidonic acid-derived prostaglandins on peripheral nociception. *J. Neuroinflamm.* **17**(1), 30 (2020).
31. Soboll, S. Regulation of energy metabolism in liver. *J. Bioenerg. Biomembr.* **27**(6), 571–582 (1995).
32. Dardevet, D., Moore, M. C., Remond, D., Everett-Grueter, C. A. & Cherrington, A. D. Regulation of hepatic metabolism by enteral delivery of nutrients. *Nutr. Res. Rev.* **19**(2), 161–173 (2006).
33. Beaupere, C., Liboz, A., Feve, B., Blondeau, B. & Guillemain, G. Molecular mechanisms of glucocorticoid-induced insulin resistance. *Int. J. Mol. Sci.* **22**(2), 623 (2021).
34. Shimba, A., Ejima, A. & Ikuta, K. Pleiotropic effects of glucocorticoids on the immune system in circadian rhythm and stress. *Front. Immunol.* **12**, 706951 (2021).
35. Kalinski, P. Regulation of immune responses by prostaglandin E2. *J. Immunol.* **188**(1), 21–28 (2012).
36. Pu, W. & Zhou, B. Hepatocyte generation in liver homeostasis, repair, and regeneration. *Cell Regen.* **11**(1), 2 (2022).

37. Wang, M. J. et al. The double-edged effects of IL-6 in liver regeneration, aging, inflammation, and diseases. *Exp. Hematol. Oncol.* **13**(1), 62 (2024).

Author contributions

Chang Liu contributed to design the study and write the manuscript. Junlong Xue collected the samples and analyzed the data. Dalong Zhu performed experiment. Alimu Tulahong helped in manuscript editing. Tuerganaili Aji drafted and revised the manuscript. All authors read and approved the final manuscript.

Competing interests

The authors declare no competing interests.

Additional information

Supplementary Information The online version contains supplementary material available at https://doi.org/10.1038/s41598-025-87614-3.

Correspondence and requests for materials should be addressed to T.A.

Reprints and permissions information is available at www.nature.com/reprints.

Publisher's note Springer Nature remains neutral with regard to jurisdictional claims in published maps and institutional affiliations.

Open Access This article is licensed under a Creative Commons Attribution-NonCommercial-NoDerivatives 4.0 International License, which permits any non-commercial use, sharing, distribution and reproduction in any medium or format, as long as you give appropriate credit to the original author(s) and the source, provide a link to the Creative Commons licence, and indicate if you modified the licensed material. You do not have permission under this licence to share adapted material derived from this article or parts of it. The images or other third party material in this article are included in the article's Creative Commons licence, unless indicated otherwise in a credit line to the material. If material is not included in the article's Creative Commons licence and your intended use is not permitted by statutory regulation or exceeds the permitted use, you will need to obtain permission directly from the copyright holder. To view a copy of this licence, visit http://creativecommons.org/licenses/by-nc-nd/4.0/.

© The Author(s) 2025